Chin. J. Astron. Astrophys. Vol. 4 (2004), No. 4, 377–389
(http://www.chjaa.org or http://chjaa.bao.ac.cn)

Chinese Journal of Astronomy and Astrophysics

Unusually Broadened Spectral Profiles Observed in Solar Prominences *

Hui Li[1], Jian-Qi You[1] and Eijiro Hiei[2]

[1] Purple Mountain Observatory, Chinese Academy of Sciences, Nanjing 210008; lihui@mail.pmo.ac.cn
[2] National Astronomical Observatory of Japan, Mitaka, Tokyo 181-8588, Japan

Received 2003 December 26; accepted 2004 February 16

Abstract After surveying the spectra of 39 prominences observed by the Multichannel Infrared Solar Spectrograph at Purple Mountain Observatory and the 25 cm coronagraph at the Norikura Solar Observatory, we found that about 28% of them show small spatial scale ($6'' - 8''$) and short time scale (tens of seconds to a few minutes), unusual large broadening and large shift velocities in spectral lines including Hα, Hβ, Hϵ, Ca II H, Ca II K, Ca II 8542 Å, He I D3 and He I 10830 Å. We present in detail two typical events observed respectively on 2002 May 27 and 1981 August 2. The full-width at half maximum of the widest profile of the 2001 prominence is 1.8 Å for Hα and 2.9 Å for He I 10830 Å, while that of the 1981 prominence is 5.3 Å for Hβ, 3.6 Å for Ca II K, 4.0 Å for Ca II H and 2.8 Å for He I D3. Such broadenings generally occur at a level of several-thousand kilometres above the chromosphere. Further, most of these prominences manifest a rotation of $(0.4\text{–}1.35)\times10^{-2}$ rad s^{-1} pointing to the Sun and large line-of-sight velocities of 20–200 km s^{-1} . Some of these events correspond in time to an enhancement or a small peak in the GOES X-ray flux, indicating the existence of high energy process at work. These prominences generally display discernible changes in the Hα morphology around the time of large broadening, but do not show Hα brightening or overall eruption except for a few small surge-like events, hence, they are hardly observed in daily Hα patrols. According to the characteristics of their Hα structures and spectral properties, we infer these events are small-scale eruptions similar to nano-flares, which may contribute to the mass and energy transported into the corona. Large turbulent velocities of 25–120 km s^{-1} are responsible for the observed broadenings.

Key words: Sun: prominences — line: profiles — turbulence

* Supported by the National Natural Science Foundation of China.

1 INTRODUCTION

Solar prominence, which can be defined as any cloud of material visible in Hα above the solar surface, has been studied extensively in the astrophysical literature (Jones 1958; Jefferies & Orrall 1963; Hirayama 1985; Heinzel & Rompolt 1987; Tandberg-Hanssen 1995; Chang & Deming 1996; Karlický et al. 2001; Gouttebroze & Heinzel 2002; Gopalswamy et al. 2003). The early studies of prominences are mainly in optical and some near ultraviolet lines such as Ca II K and the Balmer decrement of hydrogen. It was subsequently extended to near infrared lines, such as Ca II 8542 Å (Gouttebroze & Heinzel 2002) and He I 10830 Å (Landman 1976; Chang & Deming 1996), and mid-infrared lines (Zirker 1985). Recently more studies have been carried out in the extreme ultraviolet (EUV) waveband (Harrison et al. 2001; Patsourakos & Vial 2002, and references therein).

The parameters of solar prominences obtained so far are not precise, for example, Patsourakos & Vial (2002) suggested a temperature range of 5000–15000 K and an electron density range of 1.3×10^{9}–3×10^{11} cm^{-3} . Meanwhile, there are still some conflicts among the existing results. Jefferies & Orrall (1962) argued that the temperature of the region emitting He I lines must be greater than 11000 K, while the line widths of neutral hydrogen lines showed an atom temperature of about 8200 K and gave little evidence for temperature above 10000 K. Chang & Deming (1996) derived a lower helium temperature of (5300±200) K and a higher hydrogen temperature of (10900±1900) K. It was also argued whether a prominence has a cool center and a hot edge, although later works favoured such a scenario (Hirayama 1978; Hirayama 1985; Zhang & Fang 1987; Tandberg-Hanssen 1995; Chang & Deming 1996).

On the other hand, results for quiescent prominences are consistent, e.g., they have small motions of 2–10 km s^{-1} (Engvold 1972; Zhang et al. 1987; Zirin 1988). Semi-empirical models (e.g. Heasley & Milkey 1978; Zhang & Fang 1987) and a standard model known as the Hvar Reference Atmosphere (Engvold et al. 1990) were proposed for quiescent prominence in the late 1980's. The results from near- and mid-infrared spectroscopic studies suggested a prominence temperature of 10000 K, a turbulent velocity of 8.4 km s^{-1} and a radial velocity of about 3.3 km s^{-1} (Zirker 1985). EUV studies gave similar results on both the horizontal and vertical motions, but a larger turbulent velocity of 26 km s^{-1} and a line shift velocity of 11 km s^{-1} at a higher temperature of $T_e = 10^5$ K (Patsourakos & Vial 2002).

Greatly broadened spectral profiles and rotational spectral structures have been observed in active prominences, including limb flares, surges and eruptive prominences (You et al. 1998; Karlický et al. 2001, 2002), which may be driven by emerging magnetic flux or injected flux (Shakhovskaya et al. 2002), and are strongly associated with CME (Andrews & Howard 2001; Hori & Culhane 2002). Karlický et al. (2001, 2002) obtained a rotational velocity of 7–60 km s^{-1} from their study of two eruptive prominences. Recently, we examined the spectra of 39 prominences (Table 1) observed in multiple wavelengths at Purple Mountain Observatory (PMO) and the Norikura Solar Observatory of the National Astronomical Observatory of Japan (NAOJ). We found that 28% of them show small spatial scale, short time scale, large line broadenings (full width at half maximum (FWHM) $\geq$ 2.0 Å for Hα, Table 1), and much larger turbulent and line-of-sight (LOS) velocities.

In this paper, we present our studies of two typical prominences one observed on 2002 May 27 and 1981 August 2, respectively. In Sect. 2, we will briefly describe the instruments and observations. We will show our results in Sect. 3. A discussion and conclusions will be given in Sect. 4.

Table 1 List of Prominences Surveyed in this Study

Date	Obs. Period(UT)	Location	Max FWHM* (Å)	Broadening	Rotation	Remarks
1981.08.02	21:09 – 00:25	north-east	5.3	large	yes	quiescent, surge, limb flare
2001.11.30	01:15 – 01:48	south-west	2.3	large	yes	quiescent
2002.01.03	04:19 – 04:58	north-west	3.1	large	no	quiescent
2002.05.27	01:19 – 02:23	north-east	1.8	moderate	yes	quiescent,surge
2002.05.31	00:01 – 00:30	south-east	2.3	large	yes	loop prominence
2002.06.18	01:40 – 02:55	north-west	3.2	large	no	arc quiescent
2002.07.06	03:12 – 03:51	south-west	1.2	small	no	quiescent
2002.07.28	05:29 – 07:50	south-west	1.3	small	no	quiescent
2002.08.04	06:51 – 07:44	south-west	2.6	large	no	quiescent
2002.08.31	06:20 – 06:53	north-east	1.9	moderate	yes	quiescent
2002.09.06	01:46 – 02:52	north-east	1.2	small	yes	quiescnet
2002.09.20	02:20 – 02:46	south-east	0.9	small	no	quiescent
2002.09.26	01:52 – 02:59	north-west	1.2	small	yes	quiescent
2002.09.29	01:10 – 01:50	south-west	2.1	large	no	quiescent
2002.10.02	02:08 – 02:40	north-east	0.9	small	no	quiescent
2002.10.09	07:32 – 08:42	south-east	1.0	small	no	quiescent
2002.10.10	07:21 – 08:27	south limb	1.1	small	no	quiescent, loop prominence
2002.10.13	01:33 – 01:53	north-east	1.2	small	yes	quiescent hedgerow
2002.10.14	01:21 – 02:54	north-east	1.4	small	yes	quiescent, loop prominence
2002.10.16	03:47 – 04:35	south-west	1.6	moderate	yes	quiescent
2002.10.25	01:23 – 01:52	south-west	1.5	moderate	yes	quiescent, jet-like
2002.11.04	02:39 – 03:23	east limb	1.1	small	no	quiescent hedgerow
2002.11.05	00:59 – 01:44	east limb	1.0	small	no	quiescent hedgerow
2002.11.11	01:35 – 02:25	south-west	3.5	large	yes	quiescent
2002.12.27	02:41 – 03:20	south-west	1.0	small	no	quiescent
2003.01.12	01:26 – 01:49	south-east	0.8	small	no	quiescent hedgerow
2003.01.13	04:30 – 04:55	east limb	1.5	moderate	yes	quiescent
2003.03.27	05:03 – 05:42	south-east	1.1	small	no	quiescent
2003.04.16	01:16 – 01:53	south-west	1.0	small	no	quiescent hedgerow
2003.05.20	01:18 – 01:58	south-east	1.3	small	no	quiescent
2003.05.31	23:12 – 23:44	south-west	1.2	small	yes	loop prominence
2003.05.31	23:26 – 01:12	north-east	2.4	large	yes	quiescent hedgerow
2003.06.12	06:51 – 07:38	north-west	2.8	large	yes	quiescent
2003.06.13	05:36 – 06:16	north-west	1.1	small	no	quiescent
2003.06.14	01:27 – 02:56	north-west	1.8	moderate	no	quiescent, jet-like
2003.09.28	01:25 – 03:10	north-east	1.4	small	no	quiescent
2003.09.30	04:21 – 04:50	south-east	1.2	small	no	quiescent
2003.10.09	01:48 – 02:24	north-east	2.3	large	no	quiescent
2003.10.15	01:23 – 01:58	south-west	0.9	small	no	quiescent

* Maximum FWHM for Hβ (1981 August 2) or Hα (other date) line.

2 OBSERVATION AND DATA REDUCTION

All the spectral data and Hα images of the 2002 May 27 prominence were observed by the Multi-channel Infrared Solar Spectrograph (MISS) at PMO (Li et al. 1999, 2002). Three AP7p scientific CCDs were used as spectral detectors in simultaneous observation of the three spectral lines Hα, Ca II 8542 Å and He I 10830 Å at respective dispersions of 0.0545Å/pixel, 0.0511Å/pixel and 0.0478Å/pixel and exposure times of 0.5s, 0.6s and 2.0s. We took a set of spectrograms at the three lines about every 3 seconds. The slit-jaw Hα images were taken by a Daystar filter with 0.5Å passband and a Mintron MTV-1881EX CCD connected to an

image grabber, which is usually used to monitor solar activities (Li et al. 2002). We corrected the observed spectral data for dark current, flat-field, scattering light and instrument profile. The observed profiles were first calibrated by solar disk-center intensity before analysis if it is necessary. The EUV data for this event are from SoHO/EIT but unfortunately there is no TRACE data available.

The prominence on 1981 August 2 was observed with the 25 cm coronagraph at the Norikura Solar Observatory of NAOJ in the period August 2, 21:09 UT to August 3, 00:25 UT. The telescope has a focal length of 8.8 m, producing a solar image of 81 mm (Hiei 1982). The Littrow spectrograph in the Coudé configuration has a focal length of 7m and Tri-X film (35 mm $\times$ 420 mm) was used as detector. The spectrograms for the different lines were taken one by one due to the limited coverage of the film. The dispersion of the observed spectrograms is 0.275Å/mm for Ca II H and Hϵ, 0.281Å/mm for Ca II K, 0.478Å/mm for Hβ and 0.421Å/mm for D lines (D1, D2 and D3). The Hα images were taken by the slit-jaw system on Kodak 2415 film (24 mm $\times$ 35 mm). The observed Hαimages and spectrogram films were scanned by a special scanner to yield digitized Hα images and spectrograms, from which we can retrieve the line profiles in the selected wave regions. For the present study, the selected regions cover the following lines: Ca II H, Hϵ, Ca II K, Hβ, He I D3, Na I D1 and D2.

3 RESULTS

We list the prominences studied in Table 1, with their locations, maximum FWHMs for Hα or Hβ and classifications. Table 1 also shows whether the spectral lines are greatly broadened (FWHM$\geq$2.0Å for Hα or Hβ) and whether there exist rotations. Due to the limited space in this paper, we will only describe the prominences of 2002 May 27 and 1981 August 2.

3.1 The Prominence of 2002 May 27

3.1.1 Evolution of Hα Structure and Spectral Characteristics

Slit-jaw Hα images in Fig. 1 show the prominence and the eruption process. The three interesting areas are marked A1, A2 and A3 in Fig. 1a. Shown in Fig. 2 are selected Hα, Ca II 8542 Å and He I 10830 Å spectrograms taken at the same time as the Hα images of Fig. 1.

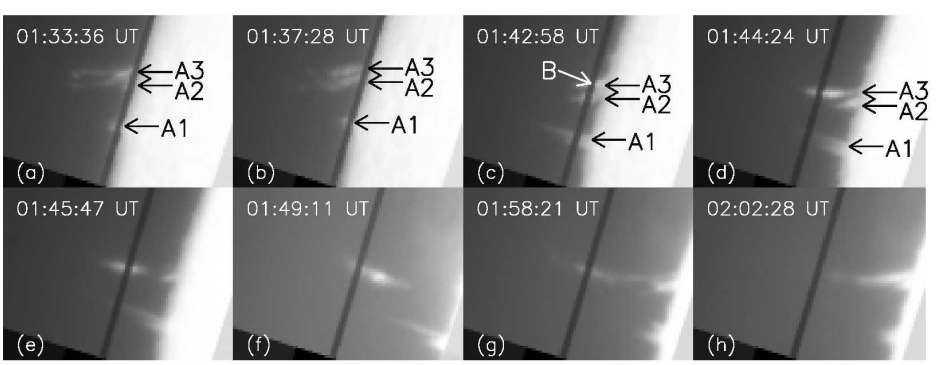

Fig. 1 Hα images of the 2002 May 27 prominence observed by the slit-jaw system of the MISS at PMO. The image size is 180″ $\times$ 135″. Observation times are noted in each image. North is on the top and east to the left. The point B in (c) marks the position where the widest profiles were observed.

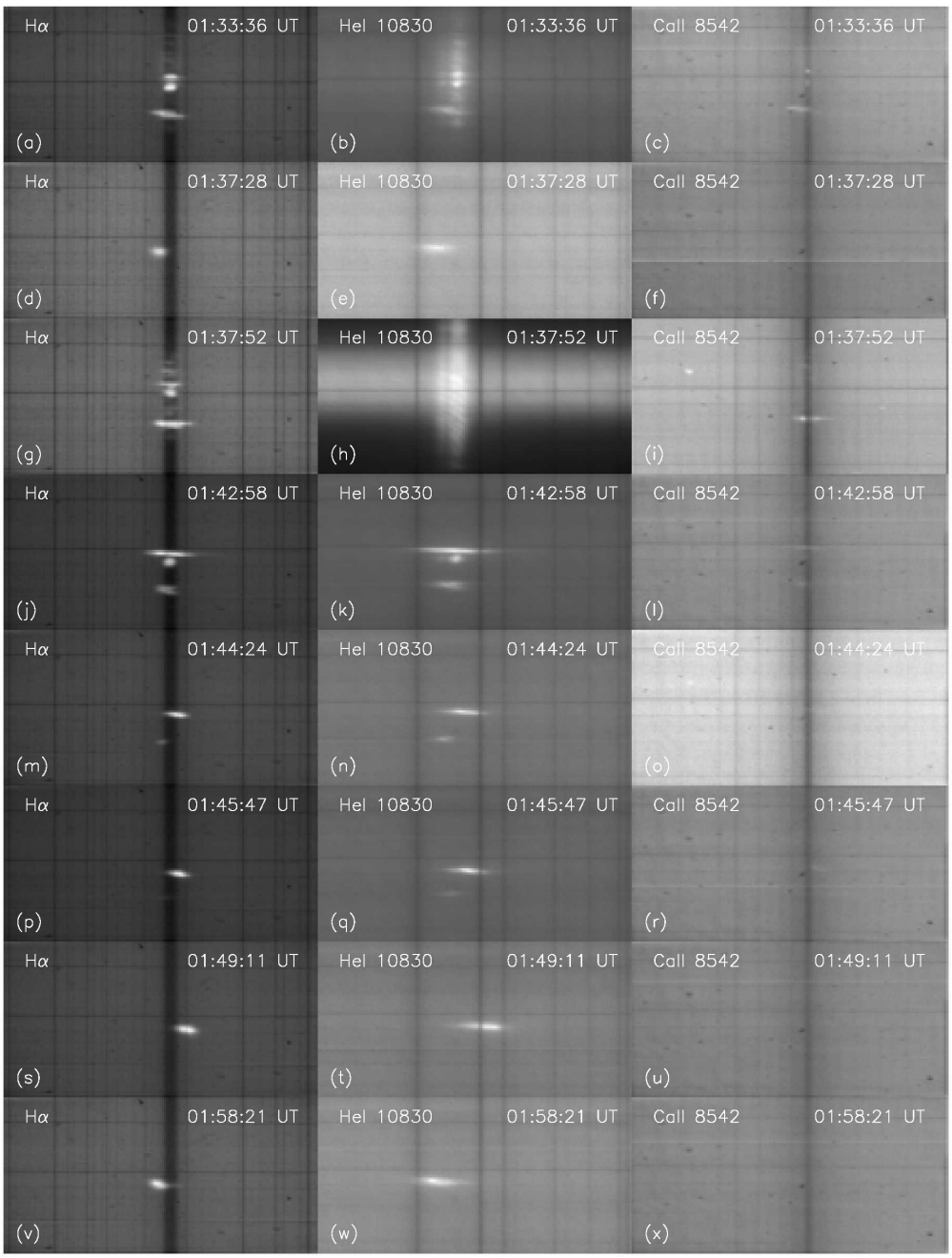

Fig. 2 Selected Hα (left), He I 10830 Å (middle) and Ca II 8542 Å (right) spectrograms corresponding to the Hα images in Fig. 1, observed by the MISS at PMO. The observation times and spectral lines are noted in each spectrogram.

At 01:33:36 UT, there was a relative stable bulge at A1 (Fig. 1a). Its spectra did not show large broadening but the tilt structure (Fig. 2a) indicates a rotational motion. The spectra at 01:37:28 UT show obvious broadening (Figs. 2d and 2e) while the Hα structure did not change (Fig. 1b). The bulge at A1 began to erupt in the Hαimage of 01:42:58 UT that now consisted of two surge-like structures. The spectra were not significantly broadened but they were blue-shifted and tilted (Figs. 2g and 2h). They remained relative stable until 01:49:11 UT (Fig. 1f), and then the northern structure began to weaken at 01:58:21 UT (Fig. 1g) and eventually faded away. The spectra at 01:44:24 UT and 01:45:47 UT were slightly blue-shifted.

There was a partially merged prominence at A2 and A3 at 01:33:36 UT (Fig. 1a) that subsequently separated into two different structures in the Hα image of 01:42:58 UT (Fig. 1c). The northern one at A3 was like a surge as a whole (Fig. 1c) and showed unusually broadened He I 10830 Å and Hα profiles (Figs. 2g and 2h), just before its eruption. After the ejection, it rose quickly with a velocity of $> 90\,\mathrm{km\ s^{-1}}$ (Figs. 1d–1g), and the broadening of the spectral lines decreased with time and the spectrum changed from being red-shifted to blue-shifted between 01:49:11 UT and 01:58:21 UT. However, tilt structures in the spectrograms suggesting a rotation pointing to the Sun were always present throughout the observation (cf. Fig. 2).

3.1.2 Observational Results

We chose the brightest part of the Hα images to measure the height of the prominence to the chromospheric limb. From the measured data in the period of 01:44:24–01:49:11 UT we determined an average rising speed of $95\,\mathrm{km\ s^{-1}}$ projected in the plane of the sky.

Our observed spectrograms showed red-shift before 01:55 UT, and then changed to blue-shift, which presumably means that the prominence plasma first moved away from, then towards, the observer. This is probably because the prominence plasma changed from rising to falling after that time. The derived line-of-sight velocity is generally 20–60 $\mathrm{km\ s^{-1}}$ (Table 2). The tilts on the observed spectrograms indicate the rotation of the rising prominence body, which is a common characteristic of eruptive prominence. The estimated rotational angular speed is about $(1.0\text{–}1.35)\times10^{-2}$ rad $\mathrm{s^{-1}}$.

Shown in Fig. 3 are the widest profiles of the three observation lines extracted from each spectrogram in Fig. 2. Figures 2 and 3 demonstrate that the emission is much weaker in Ca II 8542 Å than in Hα and He I 10830 Å. We also notice from Fig. 3 that the Hα and He I 10830 Å profiles have the same asymmetry, presumably because they come from the same source.

Apparent broadening was observed at around 01:37 UT at the bulge near A1 and around 01:43 UT at the foot part of the north prominence near A2 and A3 before the eruption. The two broadenings are different in character. The former was located at the base part of a jet and its Hα structure did show any observable change. This is similar to the brightening observed in the foot of EUV jet-like structures (Harrison et al. 2001). The latter was located in the middle part (B in Fig. 1c) and was followed by a small spray at the same time as a small increase of GOES Soft X-ray flux (Fig. 4a). However, they also have some common features: they are both small spatial scale and short time scale events and are not associated with any active region. The FWHMs of the widest Hα, He I 10830 Å and Ca II 8542 Å profiles at the latter broadening are 1.815 Å, 2.899 Å and 1.520 Å, respectively (Table 2). When taken as Gaussian profiles, the corresponding half Doppler widths are 1.090 Å, 1.741 Å and 0.913 Å. The half Doppler width of Hα is 35% smaller than the value of Karlický et al. (2002) for an eruptive prominence, while that of He I 10830 Å is about 7 times the value for a quiescent prominence given by Landman (1976).

The large Doppler widths indicate strong turbulence at the foot point of the prominence before the eruption. With the assumptions that Doppler broadening is responsible for the observed line profiles, and the Hα and He I 10830 Å are formed in the same layer (i.e., at the same temperature and turbulent velocity), we can derive the temperature (T) and the turbulent velocity (ξ) by a pair of H$\alpha$and He I 10830 Å profiles observed at the same time. The derived temperature is (11700±900) K, and the turbulent velocity is in the range 24–48 km s^{-1} (Table 2); the turbulent velocity corresponding to the widest profiles observed at 01:42:58 UT is 47.6 km s^{-1} . Here we did not use the Ca II 8542 Å profile because of its weaker emission (cf. Fig. 3). After the eruption the turbulent velocity decreased to 20–40 km s^{-1} , which is about 2–4 times the value for quiescent prominences ($\approx$ 10 km s^{-1}).

Table 2 Parameters Derived from the Observed Line Profiles of the 2002 May 27 Prominence

Wavelength (Å)	Time (UT)	FWHM (Å)	$\Delta\lambda_D$ (Å)	ξ (km s^{-1})	T (K)	$V_{\rm sh}^*$ (km s^{-1})
	01:33:36	1.031	0.619	24.3	12679	15.5
	01:42:58	1.815	1.090	47.6	12573	–15
	01:44:23	1.052	0.632	25.3	11506	–35
6563	01:45:49	1.061	0.637	26.0	10329	–26
	01:49:11	1.124	0.675	27.4	12070	–63
	01:58:21	1.116	0.670	27.5	11069	45
	01:33:36	1.523	0.915	24.3	12679	16.0
	01:42:58	2.899	1.741	47.6	12573	–13
	01:44:23	1.580	0.949	25.3	11506	–31
10830	01:45:49	1.612	0.968	26.0	10329	–28
	01:49:11	1.702	1.022	27.4	12070	–65
	01:58:21	1.700	1.021	27.5	11069	36
	01:33:36	1.189	0.714	25.0		15
8542	01:42:58	1.520	0.913	32.0		–12

* Note: positive line-of-sight velocity $V_{\rm sh}$ points to the observer.

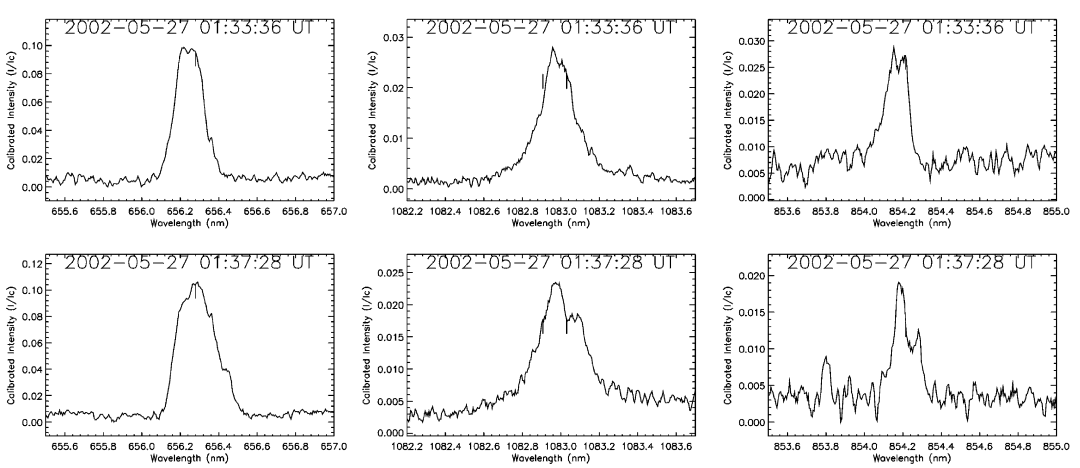

Fig. 3 Widest Hα (left), He I 10830 Å (middle) and Ca II 8542 Å (right) profiles retrieved from the spectrograms in Fig. 2. The vertical dashed bars indicate the un-shifted line centers. Ic is the disk-center intensity at nearby continuum of the corresponding wavelength.

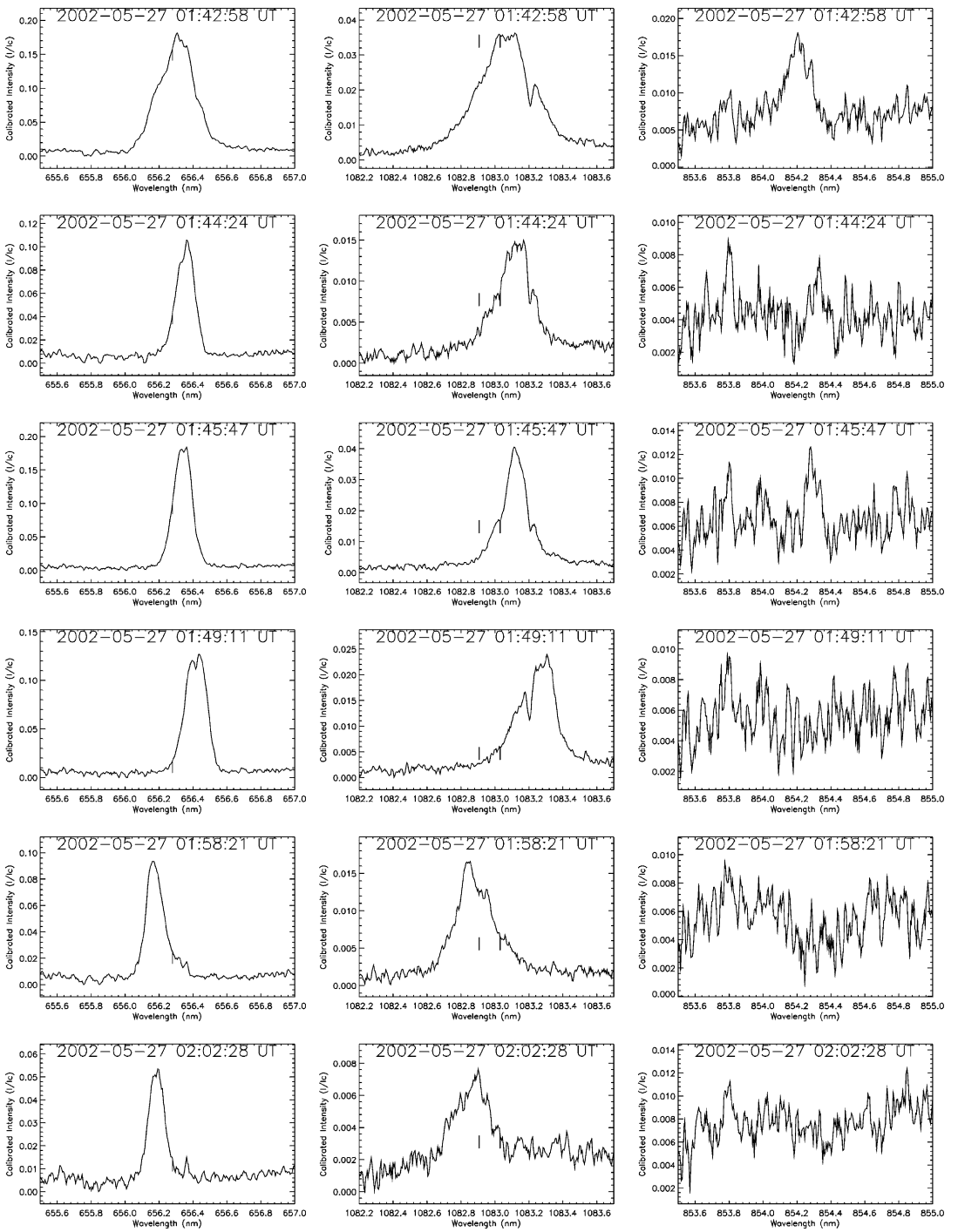

Fig. 3 Continued.

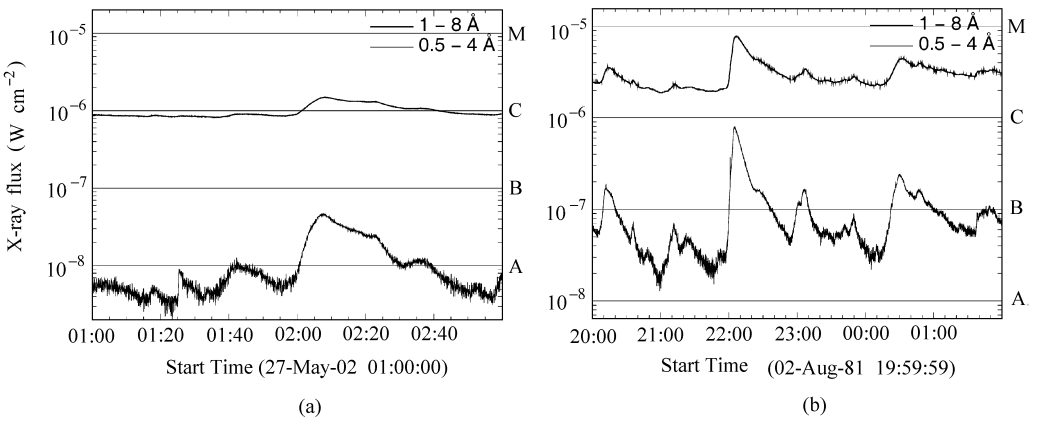

Fig. 4 X-ray curves observed by GOES for the periods of (a) 2002 May 27, 01:00 UT–03:00 UT and (b) 1981 August 2, 20:00 UT to August 3, 02:00 UT.

3.2 The Prominence of 1981 August 2

3.2.1 Evolution of Hα Structure and Spectral Characteristics

On 1981 August 2, a set of prominences were located at the north-eastern limb, spanning over an active region and a quiet area. At the beginning of the observation (21:09 UT), a rather weak prominence was located at C1 (almost undiscernible in Fig. 5a), a small bulge with a

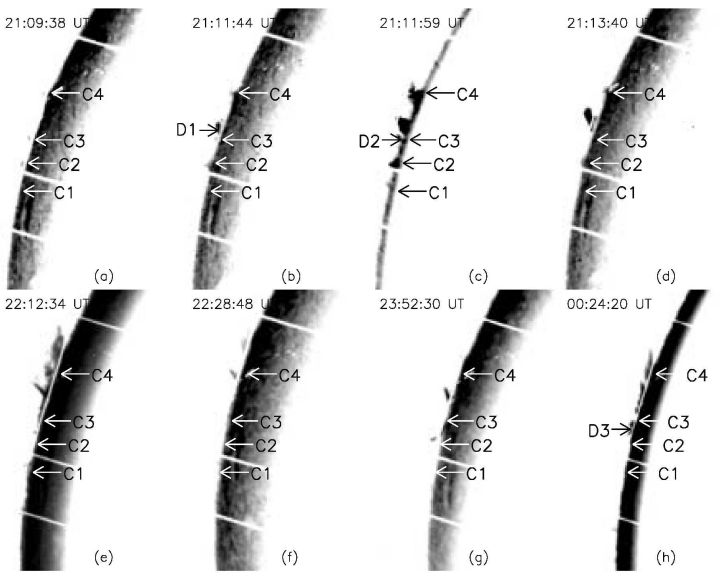

Fig. 5 Hα image of the 1981 August 2 prominence observed at Norikura Solar Observatory. The image size is $300'' \times 450''$. Observation times are noted in each image. North on top and east to the left. D1, D2 and D3 mark the positions where the large broadenings in Fig. 6(i), (m) and (h) and (l) were observed.

bright base appeared at C2. At C3, there was a small prominence-like structure, and at C4, a typical quiescent prominence. Some selected Hα images are shown in Fig. 5. The observed events mainly occurred in the four areas labelled C1, C2, C3 and C4. We will pay more attention to the quiescent prominence in C4. There was a typical hedgerow prominence north to the active region. We did not detect any broadening with velocities greater than 10 km s^{-1} at the beginning of the observation (Fig. 6a). However, 2 minutes after the occurrence of a limb flare in the southern active region, the the prominence spectra showed two filamentary broadenings with both red and blue shifts (Fig. 6b) although there was not much change in the overall structure. The redshift and blueshift velocities were as large as 175 km s^{-1} and 189 km s^{-1} , respectively. The corresponding GOES X-ray flux showed a weak increase (Fig. 4b). Thereafter, even through the prominence did not erupt (Figs. 5e) and (h)), its conformation changed to a parallel surge-like structure, and there were successive mass ejections and line broadenings (Figs. 6j and 6k).

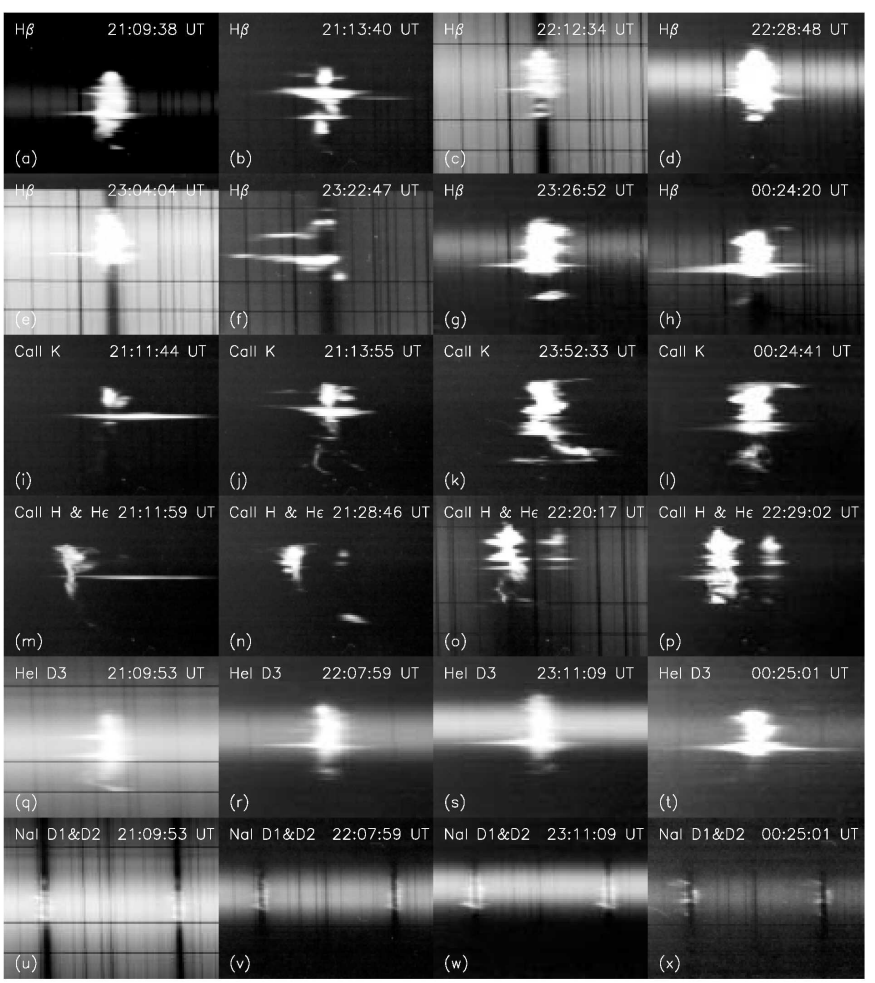

Fig. 6 Selected observed spectrograms of 1981 August 2, Hβ (row 1 and 2), Ca II K (row 3), Ca II H and Hϵ (row 4), He I D3 (row 5) and Na I D1 and D2 (last row). Observation times and lines are noted in each spectrogram.

After a limb flare took place in an area north of C3 around 21:11:44 UT (Fig. 5b), the structure of the quiescent prominence at C4 began to change, and eventually evolved into a surge-like structure (Figs. 5c–5e). Its spectra showed fibril-form broadening (Fig. 6b) and indicated a large red-shift ejecting velocity of up to 117 km s^{-1} . Broadening was observed near C2 (D1 in Fig. 5b) since the beginning (Figs. 6a, 6i and 6q). There was a mastoid on the bulge at C2 at 21:11:44 UT (Fig. 5b), whose spectra were also broadened (Fig. 6i). A large surge occurred subsequently north of the flare location before the flare completely faded away (Figs. 5c and 5d). The surge manifested large red-shift and broadening in the Ca II H and Ca II K lines (Fig. 6j).

At about 22:12 UT, a jet was ejected from the north of C3 that lasted a few minutes (Fig. 5e), around the same time as an X-ray peak (Fig. 4b). Its spectra showed broadening with less motion (Figs. 6c, 6o). A series of mastoids appeared in the Hα image near C2 around 00:24:20 of August 3 (Fig. 5h), some of which reached the height of the previous surge. Meanwhile, the widest line profiles of this prominence (D3 in Fig. 5h) were observed in these mastoids, which revealed both a large red-shift velocity of up to 359 km s^{-1} and a large blue-shift velocity of up to 225 km s^{-1} (Figs. 6h, 6i and 6t), and corresponded in time with a small X-ray peak (Fig. 4b). The base parts of these platform-like mastoids were also brightened.

Material ejections near C1 were intermittent and seemed to be related to activities near C2 and C3 (Fig. 5d). The red-shift ejection near C1 became visible and bright once there was an activity near C2 and C3. The red-shift velocity also increased up to 150–160 km s^{-1} (Figs. 6j, 6k, 6n and 6q).

3.2.2 Observational Results

Among all the observed data, there are 13 sets that have comparable Hα images and spectrograms. Two sets apart, one associated with a limb flare and one with a large surge, there are at least seven sets that are not related to generally defined active prominences (limb flare, surge and spray) but to small mastoids in the lower chromosphere and jets, they are structures not accompanied by obvious prominence eruptions. Their spectra displayed large velocities up to 117 km s^{-1} and rotational structures (Figs. 6d, 6f, 6j, 6k, 6l, 6n, 6o, 6p, 6q, 6u, 6v and 6w). All the seven sets showed significant broadening in observed spectra and/or large shift. The spectra of the surge, jet and the brightened mastoids showed large motions at the beginning which then rapidly decreased (Figs. 6b, 6c, 6i, 6j, 6m, 6n and 6r). Moreover, they showed apparent rotation towards the Sun, and the derived rotational angular speed is about 1.25×10^{-2} rad s^{-1} .

The quiescent prominence had less motion (< 10 km s^{-1}) at the beginning. However, due to the influence of the active region, it evolved into a spray structure but did not erupt, and yielded red-shifted ejections of > 100 km s^{-1} (Figs. 6k, 6l and 6o). The He I D3 line and Na I D1 and D2 lines behaved differently during the observation period. Rotational structures are obvious in the Na I D1 and D2 lines (Figs. 6u–6x), while not so significant in the He I D3 spectrograms (Figs. 6q–6t).

While all the observed events took place in the area spanning C1–C4, their individual positions were all different.

4 DISCUSSION AND CONCLUSIONS

We studied the spectra of 39 prominences observed by the MISS at PMO and the 25 cm coronagraph at Norikura Solar Observatory in daily patrol of solar activities, and presented a

detailed analysis of two typical prominences. The observations of these prominences lasted from 30 minutes to 3 hours. We found that about 28% (11 out of 39) of these prominences show large broadenings and motions of short time scale and small spatial scale. The broadenings at different positions have similar fibril structures and most but not all of the broadenings are rotational. These broadenings can occur in quiescent prominences above either active and quiet regions, although more likely in prominences above active regions. They have similar spectral properties, scales of $6''$ –$8''$, lifetimes of tens of seconds to a few minutes, and almost all of them appear at levels of several-thousand kilometers above the chromosphere. Therefore, we believe that they are events of the same kind. These broadenings are, in fact, energy release of small amount, which may be followed by GOES X-ray enhancement, mini-sprays and mini-surges. Most of them do not change the Hα morphology of the prominence.

Spectral lines displaying such broadenings include Hα, Hβ, Hϵ, Ca II H, Ca II K, Ca II 8542 Å, He I D3 and He I 10830 Å. The FWHM of the widest profile of the 2002 May 27 prominence is 1.8 Å for Hα and 2.9 Å for He I 10830 Å, while that of the 1981 August 2 prominence is 5.3 Å for Hβ, 3.6 Å for Ca II K, 4.0 Å for Ca II H and 2.8 Å for He I D3. So large broadenings could not possibly be due to thermal motion. Their most probable mechanism is strong turbulence with velocities of 25–120 km s^{-1} . We did not detect wide wings in the Na I D1 and D2 lines, probably due to their small optical thickness.

For the 2002 May 27 prominence we determined a temperature of 11700±900 K and a turbulent velocity of 24–48 km s^{-1} from the simultaneously observed Hα and He I 10830 Å profiles on the assumption that they were formed in the same layer and broadened by Doppler broadening. The inferred temperature was consistent with results of Jefferies & Orrall (1962) for neutral helium line and Chang & Deming for hydrogen line. The derived turbulent velocity is about 2–4 times the commonly accepted value for quiescent prominences, this is presumably because the prominence was partially activated. Actually, the He I 10830 Å line is formed in a layer a little higher than the Hα line, but the above assumption enabled us to determine the temperature and turbulent velocity at the same time without introducing too much inaccuracy.

We did not detect any eruption of a prominence as a whole for all these broadening events except for one case, i.e., the second event of the 2002 May 27 prominence (Figs. 1c and 1d), which showed a small spray-like ejection. Nevertheless, we often detected discernible changes in the Hα morphology around the occurrence of large broadenings. It is more interesting in the case of 1981 August 2, that whenever there was a broadening, there was a mass ejection in the vicinity of the prominence, but the prominence itself did not erupt. This is similar to the mass ejections following flares and surges, and indicates that such events are equivalent to disturbances and eruptions in a region. Because such broadenings are generally not accompanied by Hα brightening and have large line-of-sight velocities, it is difficult to detect them in routine observations of Hα, which may explain why there is no Hα counterpart for some of the GOES X-ray enhancements. However, such events may contribute to the energy and mass transported into the corona because they occur in many of the prominences (28% in our cases).

After a careful investigation of the Hα morphology of the prominences that produce large broadenings, we found that such prominences can take the form of jet-like structures, surges, semi-circle bulges and small mastoids, but do not show a preference for the form of hedgerow prominence common in quiet regions. The only broadening of hedgerow prominence in our cases was due to the influence of nearby eruptions. This implies that this type broadening may be related to the magnetic configuration below the prominence.

In addition to the large broadening, these prominences also manifest large line-of-sight ve-

locities and rotations. Large red- and blue-shift velocities can exist at the same time and can be as large as 175 km s^{-1} and 189 km s^{-1} , respectively. Tilt structures indicating rotational mass motion are also often present in the spectrograms of the studied prominences. The derived rotational angular speed is (0.4–1.35)$\times 10^{-2}$ rad s^{-1} , and points to the Sun. These suggest that rotation and large motion may be a common feature of such prominences.

Acknowledgements This work was supported by the National Natural Science Foundation of China (NSFC, grant number 10273023 and 10333040), National Basic Research Priorities Project (G2000078402) of China, and Chinese Academy of Sciences.

References

Andrews M. D., Howard R. A., 2001, Space Sci Rev., 95, 147
Chang E., Deming D., 1996, Solar Phys., 165, 257
Engvold O., 1972, Solar Phys., 23, 346
Engvold O., Hirayama T., Leroy J. L., Priest E. R., Tandberg-Hanssen E., In: Ruzdjak V., Tandberg-Hanssen E. eds., Dynamics of Quiescent Prominences, Proceedings of IAU Coll. 117, Springer-Verlag, 1990, p.294
Gopalswamy N., Shimojo M., Lu W. et al. , 2003, ApJ, 586, 562
Gouttebroze P., Heinzel P., 2002, A&A, 385, 273
Harrison R., Bryans P., Bingham R., 2001, A&A, 379, 324
Heasley J. N., Milkey R. W., 1978, ApJ, 221, 677
Heinzel P., Rompolt B., 1987, Solar Phys., 110, 171
Hiei E., 1982, Solar Phys., 80, 113
Hirayama T., 1978, In: Jensen E., Maltby P., Orrall F. eds., Physics of Solar Prominences. Inst. Theor. Astrophys., Oslo, p.4
Hirayama T., 1985, Solar Phys., 100, 415
Hori K., Culhane J., 2002, A&A, 382, 666
Jefferies J., Orrall, Q., 1962, ApJ, 135, 109
Jefferies J., Orrall Q., 1963, ApJ, 137, 1232
Jones F., 1958, J. Royal. Astron. Soc. Canada, 52, 149
Karlický M., Kotrč P., Kupryakov Y., 2001, Solar Phys., 199, 145
Karlický M., Kotrč P., Kupryakov Y., 2002, Solar Phys., 211, 231
Landman D. A., 1976, Solar Phys., 50, 383
Li H., Fan Z., You J., 1999, Solar Phys., 185, 67
Li H., You J., Wu Q., Yu X., 2002, Chin. Phys. Lett., 19, 742
Patsourakos S., Vial J.-C., 2002, Solar Phys., 208, 253
Shakhovskaya A., Abramenko V., Yurchyshyn V., 2002, Solar Phys., 207, 369
Tandberg-Hanssen E., 1995, The Nature of Solar Prominences, Dordrecht: Kluwer Academic Press
You J., Wang C., Fan Z., Li H., 1998, Solar Phys., 182, 431
Zhang Q. Z., Fanag C., 1987, A&A, 175, 277
Zhang Q. Z., Livingston W. C., Hu J., Fanag C., 1987, Solar Phys., 114, 245
Zirin H., 1988, Astrophysics of the Sun, New York: Cambridge University Press
Zirker J. B., 1985, Solar Phys., 102, 33